Short Review on Thermohydraulic Performance Enhancement of Solar Flat Plate Air Heaters Using Novel Turbulators

Sridharan M[1], *Mohammad Israr*[2]

[1&2] Lincoln University College, 47301, Petaling Jaya, Selangor Darul Ehsan, Malaysia

[2] Maryam Abacha American University of Nigeria, Kano, Nigeria

Email ID: [1] thisissridharan@gmail.com and [2] president@maaun.edu.ng

---

Abstract: Solar flat plate air heaters (SFPAHs) are extensively used for applications which demands thermal power as source. However, their thermal efficiency is mainly limited by unstable or low convective heat transfer and stable boundary layer formation along the absorber surface. This study compares and present insights from critical review on the available heat transfer enhancement methods (geometrical modifications, artificial roughness, turbulator integration etc.) of the SFPAHs. From the observed literatures, it is clearly inferred that the integration of turbulators offers significant improvement. In specific, cylindrical turbulators aligned vertical to the absorber plate recorded the best heat transfer coefficient, Nusselt Number, thermal efficiency and thermohydraulic performance factor in comparison with remaining turbulator geometries. Also, this study recommends a novel cylindrical turbulator that provides improved contact surface length and promotes repeated boundary layer redevelopment. This configuration enhances mixing and heat transfer while moderating excessive pressure drop typically associated with sharp-edged inserts.

Keywords: solar flat plate air heater; heat transfer; enhancement methods; novel turbulators; and increased contact surface length.

Introduction

A SFPAH converts incident solar radiation on it into beneficial thermal energy. This form of conversion is mainly a demand for heating applications (which requires hot air) such as space heating, crop drying, industrial preheating and greenhouse conditioning [1]. The SFPAH system basically comprises of a top layer made of transparent toughened glass as its cover, air flow channel, core absorber plate, and bottom most layer as insulation. In spite of its structural simplicity and feasibility (economic), the key restriction of the dominant SFPAHs is their comparatively poor thermal efficiency [2]. Such constraint ascends mostly due to the ineffective usage of the principle thermal power by the components of the SFPAHs. This situation leads to reduction in convective heat transfer rate. Also leads to the formation of steady thermal boundary layers along the absorber surface [3].

Researchers proposed numerous methods to augment the thermohydraulic performance of SFPAHs. They are: geometrical modifications (corrugated absorber plates, V-grooved surfaces, finned configurations, and double-pass arrangements), flow disruption techniques (rib roughness, twisted tapes, perforated baffles, and wire mesh inserts), thermal energy storage integration using Phase Change Materials (PCM), nano-enhanced PCM, and encapsulated storage units has also been explored [4]. Such methods mainly aim for improving flow interaction, increasing heat transfer area, to induce turbulence,

to disturb the laminar sublayer and also to progress energy utilization during low solar intensity periods. Among the above methods, the integration of turbulators has recorded particularly the significant thermohydraulic improvement [5]. Figure 1 presents the schematic layout of the SFPAH system with turbulators.

The superior efficiency of fore mentioned turbulators are fundamentally linked to enhanced mixing mechanisms and boundary layer disruption. Generally, in the SFPAH with flat absorber plate a thermal boundary layer develops, increases resistance (thermal) and limits rate of heat transfer [6]. The introduction of turbulators disturbs this stable thermal boundary layer development, making repeated redevelopment and thereby leads to the improved convective heat transfer coefficient (local) [7-13].

Besides, integration of turbulators creates vortices, secondary flows, and recirculation zones. This leads to the improvement in fluid mixing and the communication time between the working fluid and the heated surfaces. Definitely, the introduction of turbulators may increases hydraulic penalty (pressure drop and friction factor). The improvement in Nusselt number generally outweighs the forementioned hydraulic penalty, resulting in an enhanced thermal performance factor. Therefore, the introduction of turbulators contribute not only to thermal enhancement but also to thermohydraulic performance.

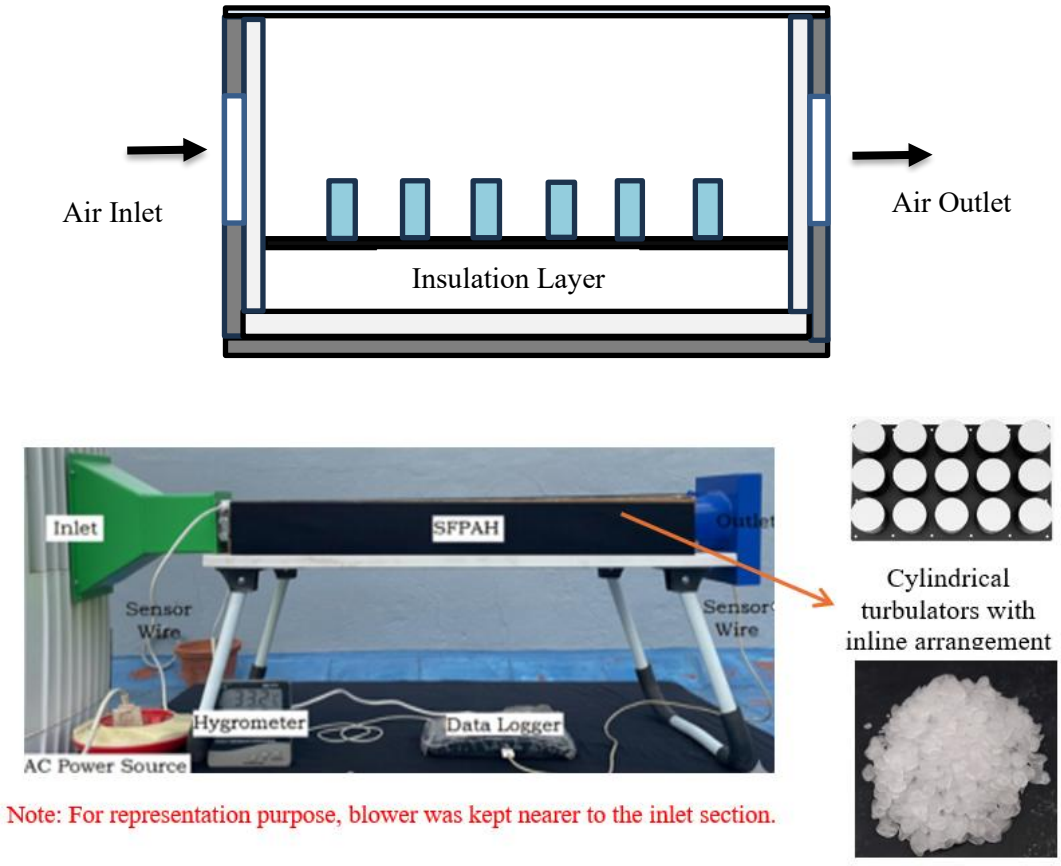

Figure 1. The schematic layout of the SFPAH system with turbulators.

Research Gap

Numerous turbulator geometries such as (cylinder, cone, pyramids etc.) have been examined to improve heat transfer enhancement and flow disturbance. Cylindrical geometries investigated by researchers include solid, perforated, hollow, corrugated, and helical structures. Conical geometries such as solid and truncated nature encourages vortex formation and gradual flow acceleration. Spherical based geometries induce isotropic disturbance patterns and wake formation. Prism based geometries including square, cubes, rectangular, and triangular leads to localized turbulence and strong flow separation. Also with the progression of additive manufacturing based technologies, configurations such as fractal geometries, louvered structures, delta winglets, and lattice-based inserts have also been sightseen. Despite these extensive investigations, optimization between heat transfer enhancement and pressure drop remains a continuing challenge.

It is clearly inferred that the numerous geometries have been reported in the literature, there remains a determined trade-off among the augmentation of heat transfer and hydraulic losses. Dominant geometries meaningfully increase the friction factor, leading to greater working fluid pumping power requirements and reduced overall efficiency. Also, certain inserts produce dead zones and non-uniform flow distribution, resulting in unstable temperature at the outlet. Dominantly available existing manufacturing techniques also limit geometric complexity, restricting the examination of multi-stage or hybrid structures. Therefore, there is a clear need for innovative turbulator geometries that can maintain high turbulence intensity while minimizing pressure penalties and ensuring uniform thermal distribution.

Materials and Methods

This section presents details related to the physical geometry involved in the CFD models (Case – 1; Case – 2; Case – 3 and Case – 4) observed. Figure 2 presents the graphical illustration of different cases of stepped cylinder observed and compared with the solid cylinder.

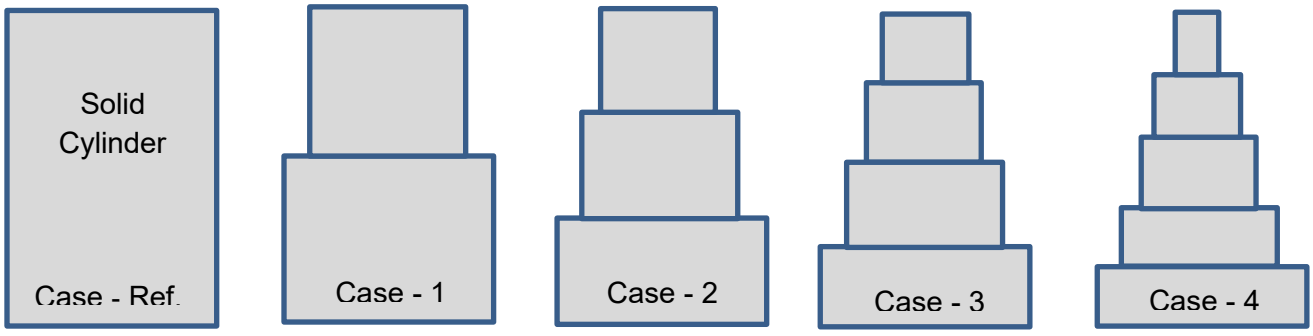

Figure 2. The graphical illustration of different cases of stepped cylinder observed and compared with the solid cylinder.

All the cases listed above in Fig. 2 are meticulously designed and simulated using ANSYS 16.0 FLUENT (computational fluid dynamics (CFD)) simulations. Among the existing cases of turbulators concern, case-4 recorded the best and balanced results in terms of thermo-hydraulic performance. This section details the procedure of the best performing geometry (case – 4) alone for the better understanding of the reader.

The considered test rig includes stepped cylinder with four turns (case – 4) and rectangular enclosure of 60 * 60 * 60 mm dimension. The novel turbulator designs were positioned perpendicular to the direction

of fluid flow to simulate normalized real-world conditions (solar irradiation and ambient temperature) from the locations of Tiruchirappalli (10.7905° N, 78.7047° E).

In the CFD simulations, the geometry was discretized into a fine computational grid using meshing techniques to ensure accurate resolution of flow features. The solid cylinder served as a baseline, while the case-4 were designed to enhance turbulence and improve heat transfer efficiency. The case-4 featured with four turns are expected to create intricate flow patterns and promoting enhanced mixing. The meshing of the geometry was performed using ANSYS FLUENT 16.0 software. Tetrahedral meshes were adopted for the computational domain, with advanced sizing functions for proximity and curvature taken into consideration. Finer meshes were applied specifically at the turbulators. The total number of mesh elements varied from 0.9 to 3.9 × 105 across different types, depending on the number of corrugations.

The numerical simulation was performed using ANSYS FLUENT 16.0 software. The fluid flow through the collectors, especially after passing over and behind the turbulators, displayed turbulent behaviour with random fluctuations in the flow variables. Table 1 lists the thermo-physical properties of the working fluid (air) and the absorber material (copper).

Turbulence modelling was employed using the k-ε (k-epsilon) model to capture the effects of turbulence on the flow and heat transfer. The ambient wind velocity, inlet mass flow rates, temperature of the air and outlet pressure are considered as 1 m/s, 0.05 kg/s, 300 K, and 0 respectively. The computational domain is established with specific boundary conditions: the inlet and outlet are designated as inlet and outflow boundaries, respectively, while the walls, including the absorber plate and the insulated wall, are treated with wall boundary conditions. The SIMPLE algorithm was utilized for pressure-velocity coupling, with pressure discretization handled using the standard scheme. For remaining variables, a second-order upwind scheme was employed to ensure best computational results. Appropriate under-relaxation parameters were implemented to achieve smooth convergence of the solution for the various variables.

Table 1. Thermo-physical properties of absorber plate, and heat transport fluid

Properties	Absorber Plate	Heat transport fluid (Air)
Density (kg/m^3)	8930	1.262
Thermal Conductivity (W/m-K)	385	0.025
Specific Heat (J/kg-K)	401	1004
Dynamic Viscosity (N/m^2-S)	N/A	$1.80*10^{-6}$
Melting Point (°C)	N/A	N/A

Physical Modelling

The computational domains for all simulation types of turbulators (with and without), were discretized into non-uniform structured elements to analyze thermohydraulic flow behaviors. The following established assumptions for SFPAC were applied in this CFD study:

1. The fluid flow is modelled as two-dimensional (2-D) and steady-state.
2. The fluid is treated as incompressible across the entire domain.
3. In all the simulation of cases, absorber plate is modelled using a thin wall assumption.
4. The thermo-physical properties of the flowing air and the absorber plate are assumed to be constant throughout the analysis.
5. Radiation losses are excluded from the analysis.

Governing Equations

The conservation of mass states that mass cannot be created or destroyed. For a fluid, the continuity equation is given by Equation 1 as in [16 and 17]

$$\frac{\partial \rho}{\partial t} + \nabla.(\rho u) = 0 \tag{1}$$

The conservation of momentum is derived from Newton's second law, which states that the rate of change of momentum is equal to the sum of the forces on a fluid element. For a Newtonian fluid, the Navier-Stokes equations are given in Equation (2) as in [15, 16 & 17]:

$$\rho\left(\frac{\partial u}{\partial t} + u.\nabla \mathrm{u}\right) = -\nabla \mathrm{p} + \mu.\nabla.\nabla.\mathrm{u} + \mathrm{f} \tag{2}$$

The conservation of energy states that the rate of change of energy in a fluid element is equal to the sum of heat added to the element and the work done on the element. The energy equation can be written as in Equation (by [16 & 17]:

$$\rho\left(\frac{\partial u}{\partial t} + u.\nabla \mathrm{e}\right) = -\nabla.\mathrm{q} + \varphi \tag{3}$$

Equation 4 presents mathematical representation for the energy equation describes the conservation of energy in the fluid and is given by [7]:

$$\rho\, c_p\left(\frac{\partial T}{\partial t} + u.\nabla \mathrm{T}\right) = -k\,\nabla^2\,\mathrm{T} \tag{4}$$

Equation 5 and 6 presents mathematical representation for the k-ϵ epsilon model includes two transport equations:

$$\frac{\partial(\rho k)}{\partial t} + \nabla.(\rho k u) = \nabla.\left(\frac{\mu_t}{\sigma_k} + \nabla \mathrm{k}\right) + G_k - \rho_\epsilon \tag{5}$$

$$\frac{\partial(\rho \epsilon)}{\partial t} + \nabla.(\rho \epsilon u) = \nabla.\left(\frac{\mu_t}{\sigma_\epsilon} + \nabla \epsilon\right) + C_{1\,\epsilon}\frac{\epsilon}{k}\,G_k - C_{2\,\epsilon}\,\rho\,\frac{\epsilon}{k} \tag{6}$$

Performance Calculation Metrics

Equation 7 by [7 & 14] presents the mathematical representation for the convective heat transfer coefficient is

$$h = \frac{Q_u}{A_s\,(T_w - T_m)} \tag{7}$$

Equation 8 by [7 & 14] presents the mathematical representation for the average Nusselt number is,

$$Nu = \frac{h * D_h}{k_{air}} \tag{8}$$

Equation 9 by [7 & 14] presents the mathematical representation for the hydraulic diameter is calculated as

$$D_h = \frac{4 * A_c}{D_{wetted}} \tag{9}$$

Equation 10 by [7 & 14] presents the mathematical representation for The friction factor is defined as

$$D_h = \frac{(\Delta P / L) * D_h}{2\,\rho\,v^2} \tag{10}$$

Equation 11 by [7 & 14] presents the mathematical expression for the thermohydraulic performance parameter is calculated as

$$THPP = \frac{Nu_{ws} / Nuwo_s}{(f_{ws} / f_{wos})^{\frac{1}{3}}} \tag{11}$$

Results and Discussion

This section presents results inferred from the computational fluid dynamics (CFD) models for the proposed stepped turbulator integrated solar flat plate air heaters (SFPAH's) with the existing turbulators in the literature. For this, variations in the outlet temperature, friction factor, pressure drop, and convective heat transfer coefficient, thermal efficiency and thermos-hydraulic performance parameters were evaluated. Table 2 presents detailed comparison of existing geometries in the literature with the proposed one.

Conclusions

The stepped cylindrical turbulator introduces axial geometric discontinuities along its length, creating multiple stages of boundary layer disruption. Each step forces flow separation and reattachment, resulting in repeated boundary layer redevelopment and enhanced local Nusselt number. Unlike sharp-edged prismatic inserts, the stepped cylindrical geometry provides relatively smoother transitions between stages, thereby moderating abrupt pressure losses while sustaining strong vortex formation. The stepped configuration also promotes controlled recirculation zones and micro-vortex generation, leading to improved mixing and more uniform outlet temperature profiles. Furthermore, the geometry is highly compatible with additive manufacturing, enabling precise control over step height, diameter ratios, and spacing, which can be further optimized using AI/ML-based predictive models. Hence, the stepped cylindrical turbulator represents a hybrid enhancement mechanism that balances thermal augmentation and hydraulic performance, offering a promising pathway for next-generation high-efficiency solar flat plate air heaters.

Table 2. Impact of different turbulators on the thermal efficiency and pressure drop in SFPAHs

Case Name & Reference(s)	Turbulator Geometry	Friction Factor	Pressure Drop (Pa)	Heat Transfer Coefficient (W/m^2K)	THPP	Thermal Efficiency (%)
Absorber Plate (Without Turbulator) & [18]		0.00907	0.0145	14.4	0.59	37
Pyramid Turbulator & [18]	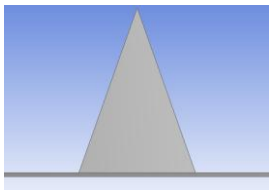	0.05021	0.1165	8	0.65	44
Spherical Turbulator & [18]	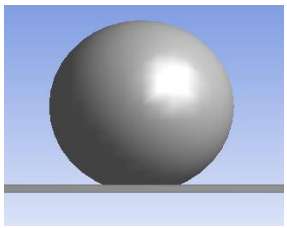	0.03800	0.0980	11.2	0.79	52
Conical Turbulator & [18]	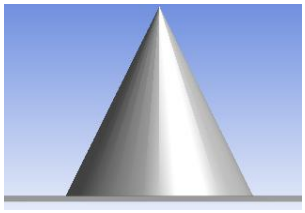	0.0.04046	0.0865	11.4	0.89	51
Hemi-Spherical Turbulator & [18]	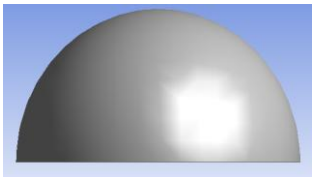	0.02360	0.0490	11.9	0.90	43
Cubical & [18]	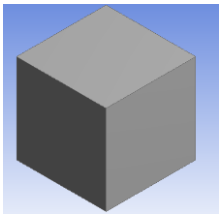	0.05223	0.1707	3.9	0.84	52

Rectangular [18]	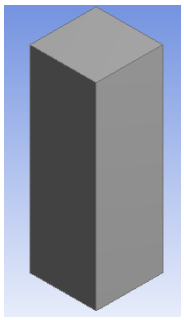	0.06223	0.1609	11.60	0.80	NR
Horizontal Cylindrical Turbulator & [18]		0.04052	0.1222	11.5	0.91	7.6
Inclined Cylindrical Turbulator & [18]	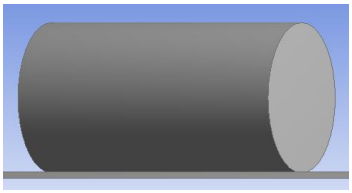	0.04118	0.1241	11.5	0.92	6.6
Vertical Cylindrical Turbulator & [18]		0.04470	0.1275	6.4	1.16	63
Stepped Cylinder & Present Study	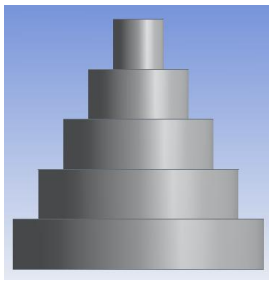	*0.04626*	*0.1309*	*15.90*	*1.29*	*70.65*

References

1. Maniyanthottil, Y. Srikanth, P. Balakrishnan, Experimental comparison of thermal, economic, and environmental outcomes in open-cut fin solar air heaters, Solar Energy 301 (2025). https://doi.org/10.1016/j.solener.2025.113992.
2. A.E. Kabeel, A. Khalil, S.M. Shalaby, M.E. Zayed, Experimental investigation of thermal performance of flat and v-corrugated plate solar air heaters with and without PCM as thermal energy storage, Energy Convers. Manag. 113 (2016) 264–272. https://doi.org/10.1016/j.enconman.2016.01.068 .
3. A. El Khadraoui, S. Bouadila, S. Kooli, A. Guizani, A. Farhat, Solar air heater with phase change material: An energy analysis and a comparative study, Appl. Therm. Eng. 107 (2016) 1057–1064. https://doi.org/10.1016/j.applthermaleng.2016.07.004 .
4. A.K. Singh, N. Agarwal, A. Saxena, Effect of extended geometry filled with and without phase change material on the thermal performance of solar air heater, J. Energy Storage 39 (2021). https://doi.org/10.1016/j.est.2021.102627 .
5. A.F. Sharol, A.A. Razak, Z.A.A. Majid, M.A.A. Azmi, M.A.S.M. Tarminzi, Y.H. Ming, Z.A. Zakaria, M.A. Harun, A. Fazlizan, K. Sopian, Effect of thermal energy storage material on the performance of double-pass solar air heater with cross-matrix absorber, J. Energy Storage 51 (2022). https://doi.org/10.1016/j.est.2022.104494 .
6. A.M. Fadhil, J.M. Jalil, G.A. Bilal, Experimental and numerical investigation of solar air collector with phase change material in column obstruction, J. Energy Storage 79 (2024). https://doi.org/10.1016/j.est.2023.110066 .
7. S.I.U. Din, A. Ibrahim, A. Fazlizan, H.A. Kazem, K. Sopian, A.B. Al-Aasam, M.A.A. Rahmat, Performance analysis of a photovoltaic double-pass solar air heater with staggered-Sandwich PCM cylinders as dual cooling and latent heat storage, J. Energy Storage 132 (2025). https://doi.org/10.1016/j.est.2025.117739 .
8. A. Hedau, S.K. Singal, Thermo-hydraulic performance investigation of double pass solar air heater integrated with PCM-based thermal energy storage, J. Energy Storage 79 (2024). https://doi.org/10.1016/j.est.2023.110202 .
9. E. Vengadesan, V. Dhinakaran, S. Senthil, P. Renugadevi, R. Senthil, Performance augmentation of solar air heater using absorber with multi-functional encapsulated PCM tubes, J. Energy Storage 72 (2023). https://doi.org/10.1016/j.est.2023.108296.

10. M. Sajawal, T.U. Rehman, H.M. Ali, U. Sajjad, A. Raza, M.S. Bhatti, Experimental thermal performance analysis of finned tube-phase change material based double pass solar air heater, Case Studies in Thermal Engineering 15 (2019). https://doi.org/10.1016/j.csite.2019.100543 .
11. P. Balakrishnan, S.K. Vishnu, J. Muthukumaran, R. Senthil, Experimental thermal performance of a solar air heater with rectangular fins and phase change material, J. Energy Storage 84 (2024). https://doi.org/10.1016/j.est.2024.110781 .
12. V. Patel, K.B. Judal, K. Sharma, M.A. Rosen, A. Kumar, M.A. Mumtaz, M.H. Elgamal, M.I. Farouk, I. Malik, Effect of channel depth ratio and absorber plate configuration on performance of a solar air heater, Case Studies in Thermal Engineering 61 (2024). https://doi.org/10.1016/j.csite.2024.104789 .
13. A. Alasiri, H.E. Fawaz, CFD investigation and ANN prediction of heat transfer coefficient for fully developed turbulent air flow around double V-baffle turbulators, Case Studies in Thermal Engineering 71 (2025). https://doi.org/10.1016/j.csite.2025.106096 .
14. M. Caner, E. Gedik, A. Keĉebaŝ, Investigation on thermal performance calculation of two type solar air collectors using artificial neural network, Expert Syst. Appl. 38 (2011) 1668–1674. https://doi.org/10.1016/j.eswa.2010.07.090 .
15. S.A. Mohammed, W.H. Alawee, A.S. Abdul-Zahra, H.S. Majdi, M.A. Fayad, M.T. Chaichan, Thermal performance enhancement of a PCM-assisted cylindrical solar air heater with moisture traps for Barhi dates drying, Case Studies in Thermal Engineering 71 (2025). https://doi.org/10.1016/j.csite.2025.106255.
16. S. Harish, D. Orejon, Y. Takata, M. Kohno, Thermal conductivity enhancement of lauric acid phase change nanocomposite with graphene nanoplatelets, Appl. Therm. Eng. 80 (2015) 205–211. https://doi.org/10.1016/j.applthermaleng.2015.01.056.
17. S.N. Dinesh, R. Saminathan, M.M. Patil, P. Ramchandra Baviskar, H. Hadidi, S. Vignesh, P. Manoj Kumar, Investigating the single pass baffled solar air heater (SAH) with an organic PCM (OPCM), in: Mater. Today Proc., Elsevier Ltd, 2022: pp. 5245–5249. https://doi.org/10.1016/j.matpr.2022.03.216.
18. Vahid Madadi Avargani, Sohrab Zendehboudi, Amir Rahimi, Sara Soltani, Comprehensive energy, exergy, enviro-exergy, and thermo-hydraulic performance assessment of a flat plate solar air heater with different obstacles, Applied Thermal Engineering, Volume 203, 2022, 117907, ISSN 1359-4311, https://doi.org/10.1016/j.applthermaleng.2021.117907 .